Unidirectional, widely-tunable and narrow-linewidth heterogeneously integrated III-V-on-silicon laser

JING ZHANG,[1,2,*] ,YANLU LI[1,2], SÖREN DHOORE[1,2] ,GEERT MORTHIER,[1,2] AND GUNTHER ROELKENS[1,2]

[1]Photonics Research Group, Department of Information Technology, Ghent University – imec, Technologiepark-Zwijnaarde 15, 9052 Ghent, Belgium
[2]Center for Nano- and Biophotonics, Ghent University, Belgium
*jingzhan.zhang@ugent.be

Abstract: A heterogeneously integrated widely tunable III-V-on-silicon ring laser with unidirectional operation is demonstrated. 40 nm tuning range (from 1560 nm to 1600 nm) is obtained using the Vernier effect between two ring resonators incorporated in the ring laser cavity. Unidirectional operation is obtained by integrating a DBR reflector coupling the clockwise and counterclockwise mode of the ring laser cavity. Unidirectional operation is obtained over the entire tuning range with about 10 dB suppression of the clockwise mode. The laser linewidth is lower than 1 MHz over the entire tuning range, down to 550 kHz in the optimum operation point. The waveguide coupled output power is above 0dBm over the entire tuning range.

OCIS codes: (000.0000) General; (000.2700) General Science.

References

1. P. Dong, X. Liu, S. Chandrasekhar, L. Buhl, R. Aroca and Y.K. Chen, "Monolithic silicon photonic integrated circuits for compact 100+Gb/s coherent optical receivers and transmitters," IEEE J. Sel. Top. Quantum Electron., **20** (4), 6100108 (2014).
2. H. Yu, M. Pantouvaki, S. Dwivedi, P. Verheyen, G. Lepage, R. Baets, W. Bogaerts, P. Absil and J. Van Campenhout, "Compact Thermally Tunable Silicon Racetrack Modulators Based on an Asymmetric Waveguide," IEEE Photon. Technol. Lett., **25**, 159-162 (2013)
3. P. P. Absil, P. Verheyen, P. De Heyn, M. Pantouvaki, G. Lepage, J. De Coster and J. Van Campenhout, "Silicon photonics integrated circuits: a manufacturing platform for high density, low power optical I/O's," Opt. Express, **23**, 9369-9378 (2015)
4. S. Tanaka, T. Akiyama, S. Sekiguchi, K. Morito, "Silicon photonics optical transmitter technology for Tb/s-class I/O co-packaged with CPU," Fujitsu Sci. Technol. J. **50**, 123–131 (2014)
5. P. Yang, S. Nakamura, K. Yashiki, Z. Wang, L. H. K. Duong, Z. Wang, X. Chen, Y. Nakamura, and J. Xu, "Inter/Intra-Chip Optical Interconnection Network: Opportunities, Challenges, and Implementations," Tenth IEEE/ACM International Symposium on Networks-on-Chip (NOCS) (2016)
6. J. Zhang, J. Verbist, B. Moeneclaey, J. Van Weerdenburg, R. Van Uden, H. Chen, J. Van Campenhout, C.M. Okwonko,X. Yin, J. Bauwelinck and G. Roelkens, "Compact Low-Power-Consumption 28-Gbaud QPSK/16-QAM Integrated Silicon Photonic/ Electronic Coherent Receiver," IEEE Photon. J., **8**, 7100110, (2016)
7. T. Komljenovic, S. Srinivasan, E. Norberg, M. Davenport, G. Fish, J. E. Bowers, "Widely tunable narrow-linewidth monolithically integrated external-cavity semiconductor lasers," IEEE J. Sel. Top. Quantum Electron., **21**, 1501909 (2015)
8. Y. Jhang, K.Tanabe, S. Iwamoto, Y. Arakawa, "InAs/GaAs quantum dot lasers on silicon-on-insulator substrated by metal-stripe wafer bonding," IEEE Photon. Technol. Lett., **27**, 875–878(2015)
9. S. Keyvaninia, M. Muneeb, S. Stankovic, R. van Veldhoven, D. van Thourhout, G. Roelkens, "Ultra-thin DVS-BCB adhesive bonding of III-V wafers, dies and multiple dies to a patterned silicon-on-insulator substrate," Opt. Mater. Express, **3**, 35–46 (2013)
10. Z. Wang, B. Tian, M. Paladugu, M. Pantouvaki, W.Guo, P. Absil, J. Dekoster, J. Van Campenhout,C. Merckling and D. Van Thourhout, "Room-temperature InP distributed feedback laser array directly grown on silicon," Nat. Photon., **9**, 837–842 (2015)
11. A. W. Fang, E. Lively, Y.-H. Kuo, D. Liang, and J. E. Bowers, "A distributed feedback silicon evanescent laser," Opt. Express, **16**, 4413-4419 (2008)

12. S. Keyvaninia, S. Verstuyft, L. Van Landschoot, F. Lelarge, G.-H. Duan, S. Messaoudene, J. M. Fedeli, T. De Vries, B. Smalbrugge, E. J. Geluk, J. Bolk, M. Smit, G. Morthier, D. Van Thourhout and G. Roelkens, "Heterogeneously integrated III-V/silicon distributed feedback lasers," Opt. Lett., **38** (24), 5434-5437 (2013)
13. S. Keyvaninia, S. Verstuyft, S. Pathak, F. Lelarge, G.-H. Duan , D. Bordel, B. Smalbrugge, E. J. Geluk, J. Bolk, J. Bolk, M. Smit, G. Roelkens, D. Van Thourhout, "III-V-on-silicon multi-frequency lasers," Opt. Express, **21**, 13675-13683 (2013)
14. J. C. Hulme, J. K. Doylend, and J. E. Bowers, "Widely tunable Vernier ring laser on hybrid silicon," Opt. Express, **21**, 19718-19722 (2013)
15. T. Segawa, S. Matsuo, T. Kakitsuka, T. Sato, Y. Kondo, and H. Suzuki, "Full C-Band Tuning Operation of Semiconductor Double-Ring Resonator-Coupled Laser With Low Tuning Current," IEEE Photon. Technol. Lett., **19**, 1322-1324 (2007)
16. G. H. Duan, C. Jany, A. Le Liepvre, A. Accard, M. Lamponi, D. Make, P. Kaspar, G. Levaufre, N. Girard, Franc, F. Lelarge, J. M. Fedeli, A. Descos, B. B. Bakir, S. Messaoudene, D. Bordel, S. Menezo, G. De Valicourt, S. Keyvaninia, G. Roelkens, D. Van Thourhout, D. J. Thomson, F. Y. Gardes, and G.. T. Reed, "Hybrid III–V on Silicon Lasers for Photonic Integrated Circuits on Silicon," IEEE J. Sel. Top. Quantum Electron., **20**, 6100213 (2014)
17. W. D. Sacher, M. L. Davenport, M. J. R. Heck, J. C. Mikkelsen, J. K. S. Poon, and J. E. Bowers, "Unidirectional hybrid silicon ring laser with an intracavity S-bend," Opt. Express, **23**, 26369-26376 (2015)
18. P. Goldberg, P. W. Milonni, and B. Sundaram, "Theory of the fundamental laser linewidth," Phys. Rev. A **44**, 1969‑1985 (1991)
19. M. C. Wu, Y. H. Lo, and S. Wang, "Linewidth broadening due to longitudinal spatial hole burning in a long distributed feedback laser," Appl. Phys. Lett. **52**, 1119‑1121 (1988)
20. M. J. Strain, G. Mezősi, J. Javaloyes, M. Sorel, A. Pérez-Serrano, A. Scirè, S. Balle, J. Danckaert, and G. Verschaffelt, "Semiconductor snail lasers," Appl. Phys. Lett., **96**, 121105 (2010)
21. P. Mechet, S. Verstuyft, T. de Vries, T. Spuesens, P. Regreny, D. Van Thourhout, G. Roelkens, and G. Morthier, "Unidirectional III-V microdisk lasers heterogeneously integrated on SOI," Opt. Express, **21**, 19339-19352 (2013)
22. D. Vermeulen, Y. De Koninck, Y. Li, E. Lambert, W. Bogaerts, R. Baets, and G. Roelkens, "Reflectionless grating couplers for Silicon-on-Insulator photonic integrated circuits," Opt. Express, **20**, 22278-22283 (2012)
23. G. Morthier, P. Mechet, "Theoretical analysis of unidirectional operation and reflection sensitivity of semiconductor ring or disk lasers," IEEE J. Quantum Electron., **49**, 1097- 1100 (2013)
24. G. Roelkens, A. Abbasi, P. Cardile, U.D. Dave, A. De Groote, Y. De Koninck, S. Dhoore, X. Fu, A. Gassenq, N. Hattasan, Q. Huang, S. Kumari, S. Keyvaninia, B. Kuyken, L. Li, P. Mechet, M. Muneeb, D. Sanchez, H. Shao, T. Spuesens, A. Subramanian, S. Uvin, M. Tassaert, K. Van Gasse, J. Verbist, R. Wang, Z. Wang, J. Zhang, J. Van Campenhout, X. Yin, J. Bauwelinck, G. Morthier, R. Baets, and D. Van Thourhout, "III-V-on-Silicon Photonic Devices for Optical Communication and Sensing," Photon., **2** (3), 969-1004 (2015)
25. C. H. Henry, "Theory of the Linewidth of Semiconductor Lasers" IEEE J. Quantum Electron. **QE-18**, 259 (1982)
26. R. F. Kazarinov and C. H. Henry "The relation of line narrowing and chirp reduction resulting from the coupling of a semiconductor laser to a passive resonator," IEEE J. Quantum Electron., **QE-23**, 1401-1409 (1987)
27. G. Morthier, K. David, R. Baets, "Linewidth rebroadening in DFB lasers due to the bias dependent dispersion of feedback," Electron. Lett., **27,** 375-377 (1991)

1. Introduction

Silicon photonics is emerging as a key photonic integration platform for the realization of advanced optical transceivers [1]. This is mainly because of the compatibility with CMOS fabrication technology, resulting in low-cost high-volume production of such circuits. Also, the large refractive index contrast available on the silicon-on-insulator platform leads to efficient active devices [2] and compact photonic integrated circuits [3]. Silicon photonic transceivers are being developed both for short reach optical interconnects in the datacenter [4-5], mostly using intensity modulation, as well as for coherent optical communication for metro-network links [6]. In both cases there is a need to integrate a III-V laser source onto the silicon photonic platform, as group IV semiconductors do not provide efficient light generation. Several approaches are being followed to realize this III-V integration, including flip-chip integration [4], bonding [7-9] or hetero-epitaxial growth [10]. Heterogeneous integration by means of molecular or adhesive die-to-wafer bonding provides a scalable approach to integrate III-V opto-electronic components on the silicon photonics platform. Several types of laser sources have been realized on this platform, including single

wavelength distributed feedback lasers [11-12], multi-wavelength lasers [13] and widely tunable lasers [7, 14, 15, 16]. In this paper we present a novel type of widely tunable laser. It comprises a ring laser cavity with integrated micro-ring resonators for the wavelength selection and it uses feedback from a Bragg grating to obtain unidirectional operation. Unidirectional ring laser structures have distinct advantages over classical standing wave ring geometries: they allow for a higher optical output power in a single output waveguide, since either the clock-wise (CW) or counter-clockwise (CCW) ring laser mode is suppressed [17]. A narrower linewidth can be achieved because of the absence of spatial hole burning [18-19], together with a more smooth output power versus wavelength characteristic, as there is no competition between the CW and the CCW mode. For these reasons several methods have been evaluated to reach unidirectional lasing, including the use of an S-bend waveguide structure inside the ring laser cavity [17], a snail shape laser [20] or an external reflector coupling the CW and the CCW mode [21]. The latter approach is followed in this paper. We report on the design, fabrication and characterization of such a widely tunable III-V-on-silicon unidirectional laser. A tuning range of 40 nm is obtained, with a suppression of the CW mode by 10dB. The waveguide-coupled output power varies between 1.5 and 3.3 mW over the tuning range, and the laser linewidth is consistently below 1 MHz, reaching 550 kHz in the middle of the tuning range. This enables the use of such a source in a master oscillator power amplifier configuration for fully integrated silicon photonics coherent transceivers for metro applications. To the best of our knowledge it is the first demonstration of an integrated widely tunable unidirectional ring laser.

2. III-V-on-silicon laser design and fabrication

The III-V-on-silicon laser cavity structure is shown in Fig. 1. It is a ring laser cavity that is formed using two micro-ring resonators with a III-V gain section in between. The silicon waveguide structures are realized using 193 nm deep-UV lithography and a 180 nm dry etch on a 400 nm thick silicon device layer. The buried oxide layer thickness is 2 μm. The ring resonator structures have a ring radius of 25 μm and 27 μm, resulting in a free spectral range of 4.1 nm and 3.7 nm respectively in the 1550 nm wavelength range. The gap between the ring resonator waveguide and bus waveguide (both 650 nm wide) is 300 nm. The distance between both ring resonators is 3 mm. Out-coupling is realized using a directional coupler structure. The length of the directional coupler is 15 μm and the gap is 350 nm, leading to a coupling of 45 % to 50 % in the 1560nm to 1600nm wavelength range (i.e. the tuning range of the presented device). Fiber-to-chip grating couplers are used to interface with optical fiber. A reflectionless grating coupler similar to the design described in [22] with low back-reflection is used. To efficiently couple light between the bonded III-V waveguide layer and the silicon waveguide layer an adiabatic coupling structure is used. Details on this adiabatic coupling structure can be found in [12]. TiAu micro-heaters are integrated on the ring resonators for wavelength tuning. Using the Vernier effect of both ring resonators a wide tuning range of 40 nm is obtained. A phase section is incorporated in the laser cavity by adding a micro-heater on top of the silicon waveguide in between the two ring resonators. In order to realize unidirectional operation a DBR grating is incorporated in the laser structure as schematically shown in Fig. 1.
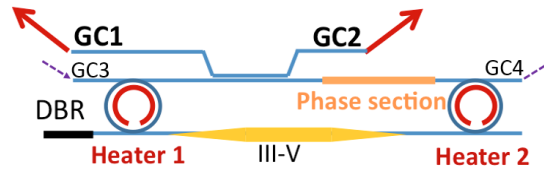

Fig. 1. Schematic of the unidirectional, widely-tunable and narrow-linewidth III-V-on-silicon laser.

This DBR is etched 180 nm deep, has a grating period of 255 nm and consists of 30 periods. The simulated reflectivity is above 90% in the 1560 nm to 1600 nm wavelength range, as shown in Fig. 2. With 30 periods the grating reflectivity saturates, providing a 3dB bandwidth of over 100 nm and a center wavelength at 1560 nm. A Focused Ion Beam (FIB) cross-section of the realized DBR is shown in Fig. 2(b).

We previously demonstrated the use of a DBR grating to couple the CW and CCW mode and thereby obtaining unidirectional operation in single wavelength micro-disk lasers as described in [21]. The theory behind the unidirectional behavior of such laser cavities is explained in [23]. In essence, by introducing the DBR, light from the CW propagating mode is coupled into the CCW propagating mode, while no light is coupled from the CCW propagating mode to the CW propagating mode. Because of gain compression, the bidirectional mode (mainly CW, but with a CCW component) has a lower gain than the unidirectional CCW mode and it is the CCW mode that thus will be lasing. No phase tuning is needed in the feedback section for the unidirectional operation [23], and thereby operation of the feedback mechanism over a broad wavelength range can be expected.
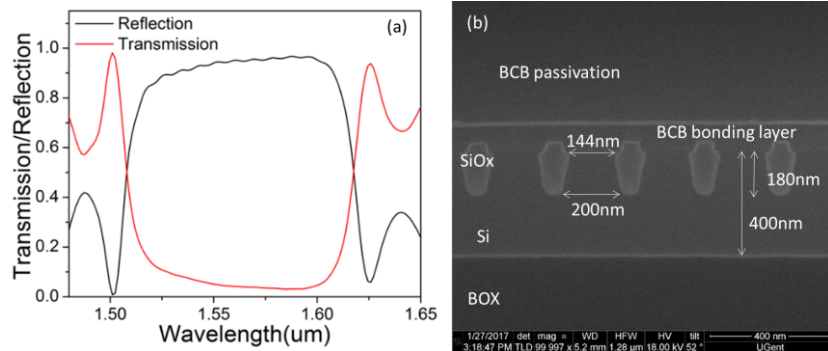

Fig. 2 (a) Simulated reflection and transmission spectrum of the used DBR. (b) FIB cross-section of the DBR.

The silicon waveguide circuits are planarized using SiO_2 and chemical mechanical planarization (CMP) down to the silicon device layer, using the SiN hard mask as the polish stop, which is afterwards removed using a hot phosphoric acid wet etch. The III-V layer stack is bonded to the silicon photonic IC using a 60 nm thick DVS-BCB bonding layer. Details on the bonding process can be found in [24]. The III-V epitaxial layer stack that is used consists of a 200 nm thick n-InP contact layer, two 100 nm thick InGaAsP separate confinement heterostructure layers (bandgap wavelength 1.17 μm), 6 InGaAsP quantum wells (6 nm thick, emission wavelength 1.55 μm) surrounded by InGaAsP barriers, a 1.5 μm thick p-InP top cladding (graded doping from $5x10^{18}$ cm^{-3} to $5x10^{17}$ cm^{-3} at the active region) and a 300 nm heavily doped p-InGaAs contact layer. The III-V gain section is 400 μm long, excluding the 180 μm long adiabatic tapers for coupling to the silicon waveguide layer. The III-V mesa is 3.2 μm wide in the gain section. A detailed process flow of the III-V membrane structure is described in [24]. In Fig. 3 a microscope image of 4 fabricated lasers is shown. The III-V-on-silicon gain section, micro-ring resonators, phase section and output grating couplers (GC1 and GC2) are indicated. The DBR grating and the output directional coupler cannot be seen in this figure as they are covered with metal traces. As the silicon waveguides are difficult to discern from the microscope image, black traces are overlaid for one of the lasers.
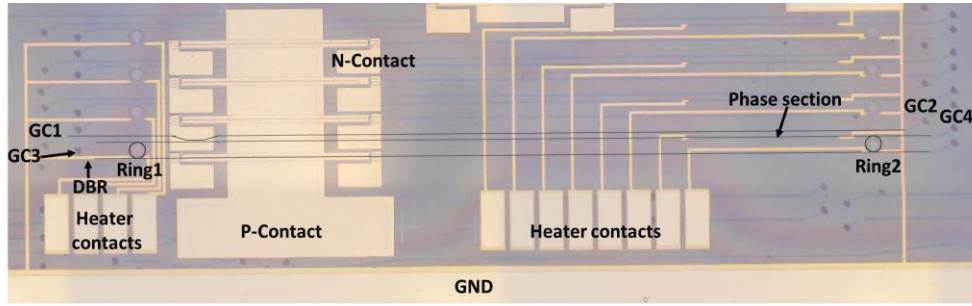
Fig. 3 Microscope image of the fabricated III-V-on-silicon laser structures, with the different building blocks indicated.

A zoom-in on the thermally tuned ring resonators and a scanning-electron microscope image of the cross-section of the III-V-on-silicon waveguide structure is shown in Fig. 4. The latter image shows the good alignment between the III-V waveguide structure and the underlying silicon waveguide.
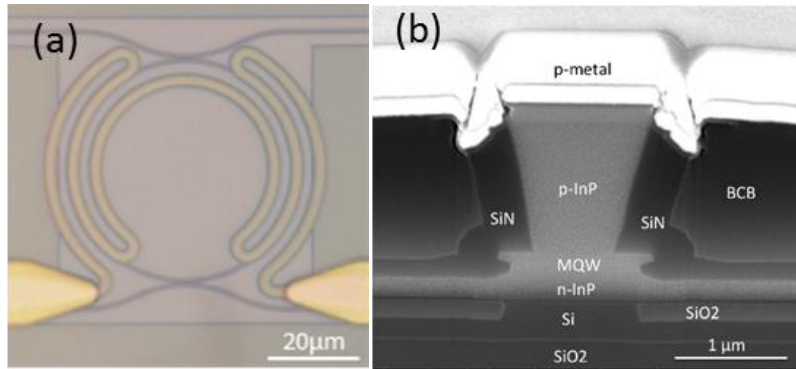

Fig. 4 (a) Microscope image of the ring resonator with a TiAu micro-heater to tune the emission wavelength; (b) SEM cross-section image of the III-V-on-silicon waveguide structure in the middle of taper section showing good alignment between the III-V waveguide and the underlying silicon waveguide

3.   III-V-on-silicon laser characterization

3.1 Ring resonator characterization

As a first step, the ring resonator structures are characterized, as shown in Fig. 5. As discussed above, the ring resonators have a slightly different radius (25 µm and 27 µm) in order to implement the Vernier tuning. The rings have a loaded Q-factor of ~ 17000 and a drop port loss of around 1 dB across the 1560 to 1600 nm wavelength range. The extinction ratio of the ring resonators is around 20 dB in the wavelength range of interest. The measured free spectral range is 4.1 nm and 3.7 nm for the 25 µm and 27 µm radius device respectively. Fig. 5(b) shows the normalized transmission spectrum of the two ring resonators by measuring the transmission from GC3 to GC4 as indicated in Fig. 1 and Fig. 3. Two sets of resonances can be observed that occasionally overlap with each other. A combined $FSR = FSR1{\times}FSR2/(FSR1-FSR2)$ of about 40 nm can be observed [15]. The low loss of the waveguide (~1 dB/cm) makes using a long passive cavity an effective way to reduce the laser linewidth [25]. In this work a cavity of 6 mm excluding the effective length introduced by the ring resonators was used. The simulated cavity roundtrip phase and the wavelength filtering effect of the two rings are shown in Fig. 5(c). The rings are assumed to be spectrally aligned and have a Q-factor of 17000. Although the phase delay in the microrings results in a

narrower longitudinal mode spacing at resonance, the full width at half maximum (FWHM) of the two-ring transmission spectrum is comparable to the longitude mode spacing, which allows for single mode operation. Moreover, if the lasing longitudinal mode is located at the longer wavelength side of the resonance peak as the right black dashed line indicates (which can be achieved by tuning the phase section) the strength of the coupling between the CW and CCW mode by the DBR can be enhanced due to the increased through port transmission of the rings, resulting in unidirectional operation. At the same time, the strong wavelength dependence of the cavity loss is helpful for narrowing the linewidth, an effect also known as detuned loading [26-27].
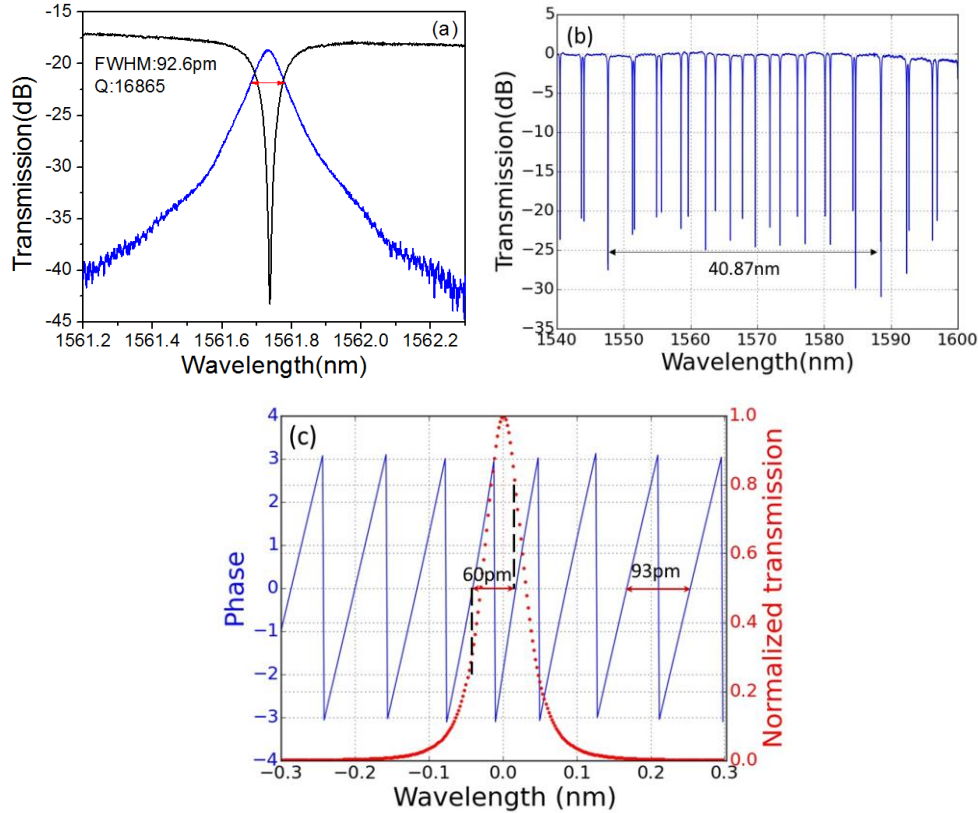
Fig. 5 (a) Representative drop port and through port transmission spectrum of the ring resonator structures. (b) Transmission of a cascade of two ring resonators with a 25 μm and 27 μm radius respectively, showing a combined FSR of about 40 nm; (c) Normalized simulated transmission of two spectrally aligned ring resonators and the cavity roundtrip phase as a function of wavelength.

3.2 Tunable laser characterization

The characterization of the tunable laser is carried out on a temperature controlled stage at 20 °C. The gain section is biased at 100 mA. The series resistance of the gain section is 10 Ω. The micro-heaters on the ring resonators have a series resistance of 5 kΩ, while that on the phase section has a series resistance of 7 kΩ. The power dissipation in the micro-heaters depends on the wavelength the laser is tuned to, but is below 50 mW per micro-heater. Fig. 6(a) shows some laser spectra overlaid, illustrating a laser tuning range of 40 nm. The output power indicated in the graph is the output power in the silicon waveguide connected to

grating coupler GC1, so generated by the CCW propagating mode. The output power varies between 1.5 and 3.3 mW over the tuning range. This smooth behavior of the output power versus wavelength is attributed to the unidirectional operation of the laser as we will discuss below. On identical devices without the DBR reflector, much larger power fluctuations were observed (> 5dB) due to the competition between the CW and CCW mode. The side mode suppression ratio is above 40 dB over the entire tuning range except for the last data point at a wavelength of 1600 nm, where it is 38 dB, as shown in Fig. 6(b).
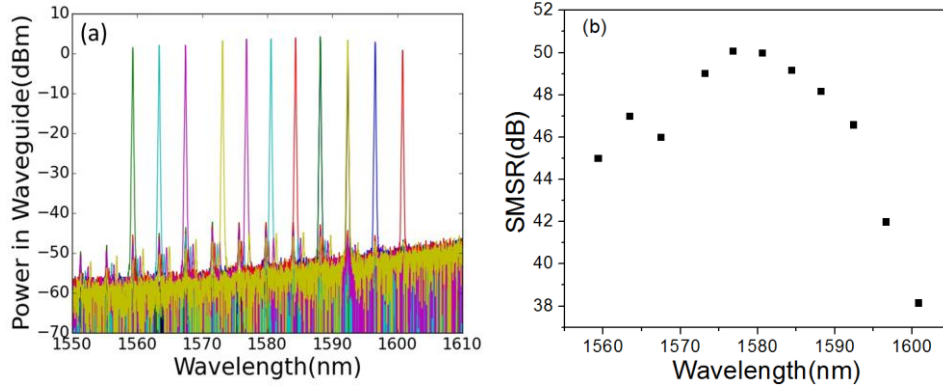
Fig. 6 (a) Overlaid output spectra of the tunable laser showing a 40 nm tuning range and smooth output power variation with wavelength. (b) Side mode suppression ratio as a function of laser emission wavelength.

The unidirectional behavior of the device is studied by simultaneously mapping the output power from GC1 and GC2. Fig. 7 shows the output power of CCW mode and the CW mode as a function of wavelength, at a laser bias current of 100 mA. The exact ratio of the CCW mode to CW mode depends on the wavelength setting, but is in the range of 10 dB. This is very different from the behavior we observed from devices without an integrated DBR, where depending on the wavelength setting either the CW or CCW mode can be dominant.
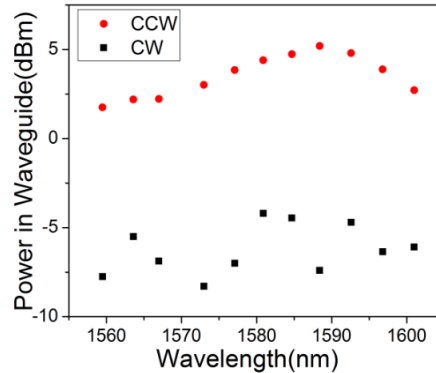

Fig. 7 Output power of the CCW and CW mode as a function of laser wavelength at 100 mA bias current.

The behavior of the device as a function of the gain section bias current was also assessed. For this the micro-heaters were driven to select a certain emission wavelength at a laser bias of 100 mA. Afterwards, the micro-heater settings were fixed and the gain section current was swept between 0 and 100 mA. In Fig. 8 the power in the CW and CCW mode is plotted as a function of gain section bias current at 4 wavelengths across the laser tuning range. As can be seen, for particular wavelengths the device behaves unidirectional from threshold up to the 100 mA bias current. At particular wavelengths bi-directional operation in the power versus

current trace can be observed over a limited current range. This behavior is attributed to the fact that in these current ranges, the longitudinal mode aligns with the resonance of the ring resonator. Given the high extinction ratio of the ring resonators and the high coupling ratio of the directional coupler (~50%), this makes the reflection from the two grating couplers dominant (measured to be ~-30 dB from optical frequency domain reflectometry in the wavelength rang of interest), causing mutual coupling between the CW and CCW mode. The reflectivity at the 500 nm wide III-V taper tip is simulated to be below -40 dB. The strong variations in the output power that can be observed are attributed to mode hops in the laser emission during bias current tuning, as is typical in this kind of laser cavities [16].
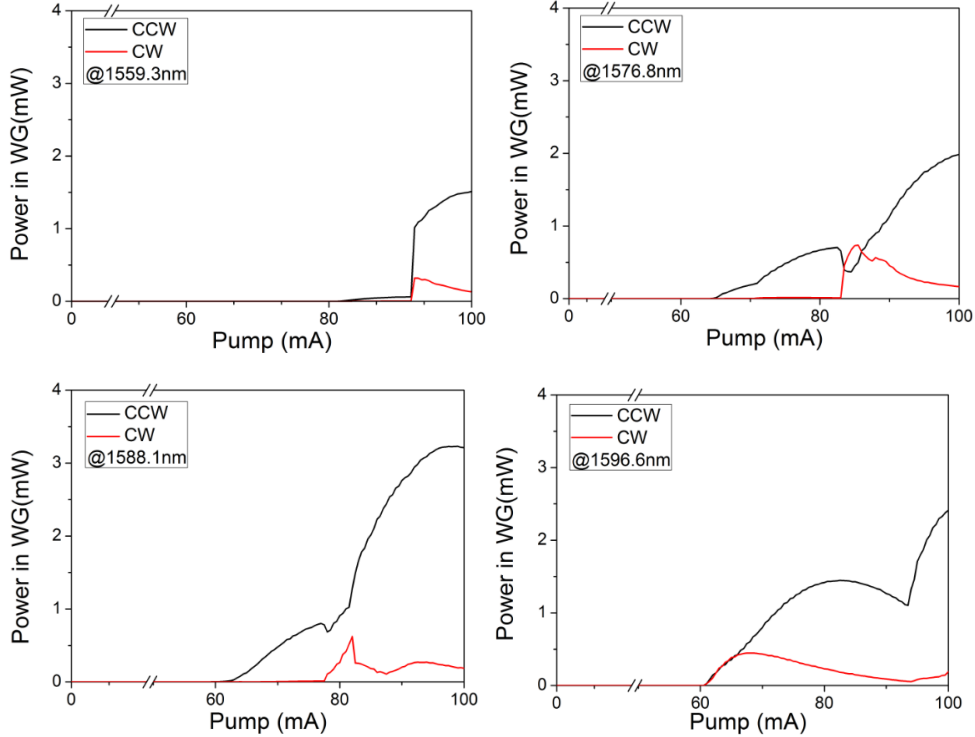

Fig. 8 Waveguide-coupled output power in the CW and CCW direction as a function of gain section bias current for different output wavelengths of the laser.

The linewidth of the laser was evaluated over its tuning range. This measurement was realized using a delayed self-heterodyne measurement, using a 200 MHz acousto-optic frequency shifter in one arm of the interferometer and a 5 km fiber delay line in the other arm. The linewidth is extracted by using a Lorentzian fitting of the beat note at 200 MHz. The result as a function of laser wavelength is shown in Fig. 9. The laser linewidth is consistently below 1 MHz and reaches 550 kHz in the optimal operation point. This enables the use of such widely tunable lasers as sources for quadrature phase shift keying (QPSK) integrated coherent transceivers.
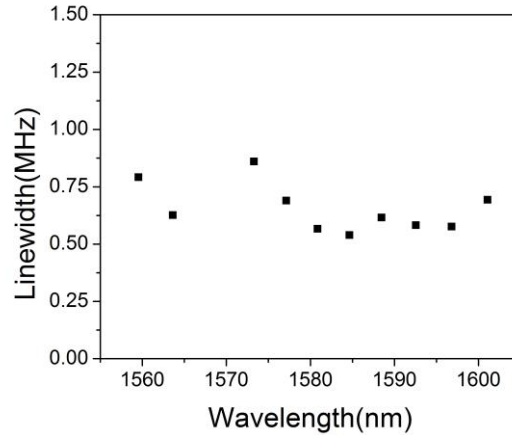
Fig. 9 Laser linewidth as a function of emission wavelength as measured using a delayed self-heterodyne measurement scheme.

4. Conclusion

In this paper we present for the first time the realization of a unidirectional, widely-tunable III-V-on-silicon ring laser. Approximately 10 dB extinction of the CW laser mode is obtained. The laser tuning range is 40 nm and the waveguide-coupled output power varies between 1.5 and 3.3 mW for a gain section bias current of 100 mA. The laser linewidth is consistently below 1 MHz enabling the use of this laser source for fully integrated QPSK coherent transceivers. The unidirectionality could be further improved by strengthening the feedback from the Bragg grating (e.g., by using microrings with a somewhat lesser extinction ratio), and by reducing the parasitic reflections from the grating couplers or their influence (e.g., by using directional couplers with lower coupling). Better unidirectionality is expected to further reduce the linewidth due to the weaker spatial hole burning effect. To further reduce the linewidth generally a higher Q ring and, under the prerequisite of single mode operation as long as possible a laser cavity could be helpful. A reduced cavity loss is required as well, as this will also increase the output power from the device.